LANGMUIR Article
Cite This: Langmuir 2019, 35, 16053−16061
pubs.acs.org/Langmuir

Comparison of Line Tension Measurement Methods for Lipid Monolayers at Liquid−Liquid Coexistence

Benjamin L. Stottrup,*[,†] Juan TigreLazo,[†] Vision B. Bagonza,[†] Joan C. Kunz,[‡] and Joseph A. Zasadzinski[§]

[†]Department of Physics and [‡]Department of Chemistry, Augsburg University, Minneapolis, Minnesota 55454, United States
[§]CEMS, University of Minnesota, Minneapolis, Minnesota 55455, United States

Supporting Information

ABSTRACT: Several methods of measuring the line tension between phase-separated liquid-ordered−liquid -disordered domains in phospholipid−cholesterol systems have been proposed. These experimental techniques are typically internally self-consistent, but the measured line tension values vary widely among these techniques. To date, no measurement of line tension has utilized multiple experimental techniques to look at the same monolayer system. Here we compare two nonperturbative methods, Fourier analysis of boundary fluctuations (BA) and one proposed by Israelachvili involving the analysis of domain size distributions (SD), to extract the line tension in a 70 mol % DMPC/30 mol % dihydrocholesterol (DChol) mixture as a function of surface pressure. We show that BA predicts the expected variation in line tension measurements consistent with the theoretical critical exponent whereas SD does not. From this comparison, we conclude that the size distribution of monolayer domains is metastable and primarily determined by the kinetics of domain nucleation and subsequent aging.

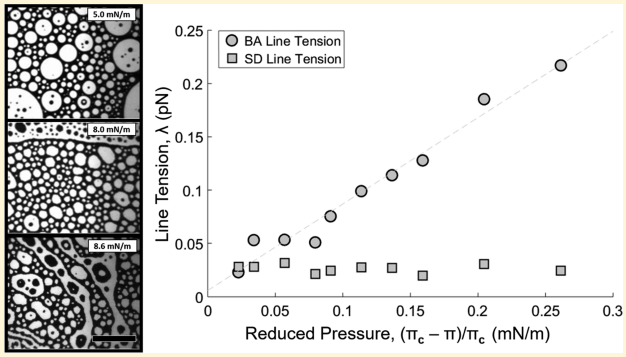

INTRODUCTION

Over the past two decades, the role of line tension in monolayers and bilayers with coexisting immiscible liquid-ordered (cholesterol-rich) and liquid-disordered (cholesterol-poor) phases has received significant attention because of the relationship between line tension and the formation and stability of lipid rafts.[1−16] The raft hypothesis postulates that submicrometer domains, or rafts, of a cholesterol-rich phase separate from a continuous, cholesterol-poor phase within the cell membrane. These physical and chemical inhomogeneities within the cell membrane provide sites for specific protein localization to carry out a host of cellular functions.[1,3,16] Stabilizing nanometer-dimension rafts likely requires a low effective line tension between the raft and the surrounding membrane, which can occur at or near a miscibility critical point.[1−16] Langmuir monolayers of phase-separated phospholipid/cholesterol mixtures provide a rich model system for studying the physical parameters determining raft formation[2,4−15,17−20] and the fundamental biophysics of coexisting immiscible liquid phases.

The line tension, λ, is the free energy per unit length of the domain boundaries in monolayers and bilayers and is the two-dimensional analog of the surface tension in three dimensions.[12,18] Differences in lipid composition, chain length, tilt, or local order at the boundaries between domains determine the magnitude of λ.[12,14,15] Increasing line tension causes the domain sizes to increase, which minimizes the ratio of domain perimeter to domain area. Opposing this line tension contribution to domain size, the head−tail asymmetry of surface-active molecules at an air−water interface leads to a net dipole moment in the direction normal to the interface.[12] Because parallel dipoles repel each other, the electrostatic energy of a domain increases with increasing domain size, counteracting the effect of the line tension. The magnitude of the dipole moment is invariably different in the coexisting phases because of differences in molecular packing, orientation, or composition, resulting in a difference in the average dipole density, μ.[12] The contribution of the dipole density difference is substantially greater in asymmetric monolayers than in symmetric bilayers, where the dipole effect of each monolayer leaflet cancels the other.

This competition between line tension at the domain boundaries and the dipole density difference between the domain and its surroundings determines the contributions of domain size and shape to the energy of each domain.[2,10−12,18,21−23] The energy per molecule, E/N, in a

Special Issue: Intermolecular Forces and Interfacial Science

Received: June 4, 2019
Revised: July 25, 2019
Published: July 25, 2019

DOI: 10.1021/acs.langmuir.9b01696
Langmuir 2019, 35, 16053−16061

noninteracting circular domain of radius r ($N = \pi r^2/a_o$, in which a_o is the average area per molecule in the domain) is set by a balance of these opposing forces:[12]

$$\frac{E}{N} = \frac{2a_o}{r}\left[\lambda - \mu^2 \ln\left(\frac{4r}{e^2\delta}\right)\right] \quad (1)$$

$\delta \approx 0.5$ nm is a molecular cutoff distance, and e is the exponential 2.714.[12] (In previous publications by Israelachvili and co-workers, the square of the dipole density difference is $\mu^2 = (\Delta m)^2/4\pi\epsilon\epsilon_o$ in SI units; ϵ is the dielectric constant of interfacial water ($\epsilon \approx 40-80$), and $\epsilon_o = 8.854 \times 10^{-12}$ C^2/N·m^2 is the permittivity of free space.) From this energy formulation, the minimum-energy radius, r_o, for noninteracting domains is

$$r_o = \frac{e^3\delta}{4}\exp\left[\frac{\lambda}{\mu^2}\right] \quad (2)$$

Equation 2 shows that increasing μ favors smaller domains and increasing λ favors larger domains. Stability analysis shows that circular domains with $r \le r_o/e$ are unstable with respect to coalescence and domains with $r \ge e^{1/3}r_o$ are unstable to elliptical or higher-order distortions.[12,24] However, this stability analysis does not provide any estimate of the rate at which the domain size distribution reaches an equilibrium value.

For lipid monolayers, line tensions are on the order of k_BT/nm, or picoNewtons, which makes direct measurement challenging.[10,12,18] The first measurements of line tension used monolayer flow[10,17−20,25,26] or micropipette aspiration[27] to modify the initial domain shape, followed by relaxation to the unperturbed shape. The line tension acts as a driving force to restore the circular domain and is resisted by the viscous drag of the subphase[20,25] or by the combination of the subphase drag and the monolayer surface viscosity.[19] This method requires some knowledge of the surface viscosity relative to the subphase viscosity, which is generally unknown, as well as a method of reversibly perturbing the interface.

Nonperturbative methods rely on the small (compared to k_BT) energy required to induce spontaneous fluctuations in domain shape and size.[12,24,28] Two such nonperturbative techniques are the analysis of domain boundary fluctuations[8,29,30] or Israelachvili's model for domain size distributions at equilibrium.[14,15] In the first method, fluctuations in the domain radius due to thermal energy can be directly related to line tension through the equipartition theorem,[8,29,30] from which the line tension[8] or the line tension and dipole density difference[29,30] can be extracted. Boundary fluctuation analysis is most accurate for low line tensions, which are more likely to be found near critical miscibility points.[12] As a practical matter, fluctuation analysis is done only for the largest domains in a monolayer, which may be problematic because domains with $r \ge e^{1/3}r_o$ are unstable to elliptical distortions, which would complicate the analysis.[12,24]

Israelachvili postulated that the domain size polydispersity observed experimentally shows that the entropy of mixing contributes to the equilibrium domain size distribution, in addition to the opposing energetics of the line tension and dipole density difference (eqs 1 and 2).[12,14,15] Combining the domain energetics of eq 1 with Israelachvili's favorite mass-action model for the mixing entropy[31] leads to a prediction for the domain size distribution. This theoretical size distribution can be fit to experimentally determined domain size distributions with the line tension and dipole density difference as adjustable parameters.[14,15] While the image processing routines necessary for evaluating domain fluctuations or size distributions are nontrivial to implement, no tools beyond fluorescence microscopy, which is already used to image the phase separation, are required. In principle, size distribution analysis can be done for any monolayer and is not restricted to near-critical mixtures as is the case for boundary fluctuation methods. However, an unresolved question is whether the experimentally determined domain size distributions are at equilibrium under the conditions of typical experiments[10,32] or are metastable distributions influenced by the monolayer history. The relatively small energy differences between domains of different radii compared to the strong electrostatic barrier to coalescence and the relatively long time scales for diffusive equilibria could trap the monolayer domains in kinetically determined size distributions, invalidating the model predictions.[33,34] This may be exacerbated for monolayers near critical points, where the line tension and dipole density differences go to zero and boundary fluctuations distort the domain shapes (Figure 1).

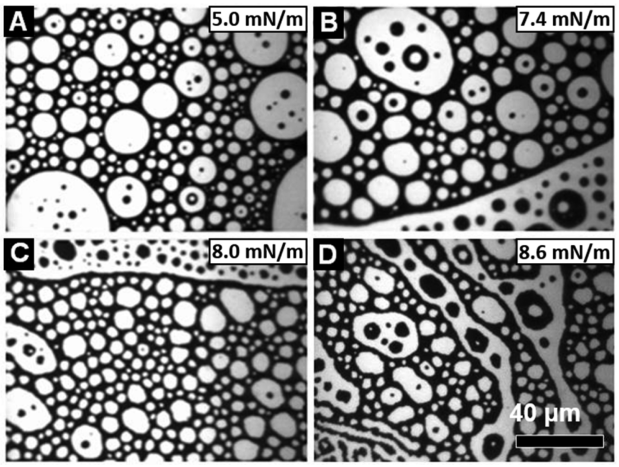

Figure 1. Fluorescence microscopy images of a 70:30 mol % DMPC/DChol monolayer at various pressures: (A) 5, (B) 7.4, (C) 8, and (D) 8.6 mN/m. Liquid-disordered (L_d) domains are bright, and the liquid-ordered (L_o) domains are dark as a result of the preferential accumulation of fluorescent Texas Red DHPE in the L_d phase. The fraction of dark and light domains is roughly 50:50 and remains constant with increasing surface pressure. Images show the increased interfacial fluctuations and circle to ellipse to stripe transition as pressures approach the critical transition pressure, $\pi_c \approx 8.8$ mN/m.

A summary of experimental techniques and values for line tension is listed in Table 1 and shows the wide range of values in the literature. The line tension in the 7:3 DMPC/cholesterol system, which is the critical composition for liquid−liquid miscibility, has been measured most often and is our choice for this comparison between methods. There are fewer measurements of the dipole density difference, μ. Benvegnue and McConnell analyzed the Brownian motion of small circular domains trapped in larger circular domains in liquid-ordered, liquid-disordered DMPC−cholesterol monolayers which gave μ ranging from 0.35 to 0.54 D/nm^2.[11] Baumgart and co-workers used boundary fluctuations to show that μ decreased from 0.68 to 0.44 D/nm^2 as the critical miscibility surface

DOI: 10.1021/acs.langmuir.9b01696
Langmuir 2019, 35, 16053−16061

Table 1. Experimental Techniques, Monolayer Compositions, and Experimental Values of Line Tension for the Three Methods Discussed in the Text[a]

monolayer composition	method of measurement	measurement value	authors	year
DMPC/Chol 7:3	monolayer flow	0.09−1.6 pN	Benvegnu et al.[10]	1992
DMPC/Chol 68:30	boundary mode	5 pN	Seul[33]	1993
8CB[b]	monolayer flow	200−600 pN	Wintersmith et al.	2007
DMPC/Chol ≈ 7:3	boundary fluctuation	0.35−1 pN	Stottrup et al.[8]	2007
DMPC/Chol ≈ 7:3	boundary fluctuation	0.15−0.6 pN	Heinrich et al.[30]	2008
nerve myelin	size distribution	0.003−0.011 pN	Lee et al.[14]	2011
lung surfactant	size distribution	0.01−0.025 pN	Dhar et al.[15]	2012

[a]The Lee and Dhar papers use the Israelachvili model for the size distribution. The 7:3 DMPC/cholesterol composition is the critical composition for liquid−liquid immiscibility. Experimental values of the line tension vary from 0.003 to 600 pN. [b]8CB is 4′-8-alkyl[1,1′-biphenyl]-4-carbonitrile.

pressure of a 70:30% DMPC/cholesterol mixture was approached from below.[30] The Israelachvili model for the domain size distribution provided estimates of μ for a model myelin monolayer composition that decreased from 0.85 to 0.45 D/nm^2 as the liquid−liquid miscibility pressure was approached from below.[14] Given the wide range of measured line tensions, the limited number of measurements of dipole density differences are quite similar among the different experimental methods. Because the average area of a phospholipid molecule is 0.40−0.8 nm^2, (depending on surface pressure) this suggests that a reasonable estimate of μ is ∼1 D per molecule.

Here we compare the Israelachvili size-distribution model (SD) to boundary fluctuation analysis (BA) to determine the line tension of the near-critical mixture of 70 mol % DMPC/30 mol % dihydrocholesterol as a function of surface pressure. For this canonical mixture, the line tension and dipole density difference have been measured by both perturbative and nonperturbative approaches (Table 1). This mixture is also the critical composition for liquid-ordered−liquid-disordered miscibility, which greatly increases the magnitude of the boundary fluctuations, making boundary analysis possible as well as providing theoretical critical exponents describing the line tension as the critical point is approached. While the approach to the critical point makes the boundary fluctuations larger and easier to analyze, it complicates the domain size distribution analysis because near the critical point domains often are far from circular (Figure 1). We find that the boundary analysis method gives line tensions that show the expected variation with surface pressure, consistent with the theoretical critical exponent, while SD provides much lower values that do not scale with surface pressure. From this comparison, we conclude that the size distribution of monolayer domains during isotherm recording is metastable and determined by the kinetics of domain nucleation and can be modified by subsequent nucleation events.

MATERIALS AND METHODS

Materials. 1,2-Dimyristoyl-*sn*-glycero-3-phosphocholine (DMPC), 1,2-dilauroyl-*sn*-glycero-3-phosphocholine (DLPC), 1,2-didecanoyl-*sn*-glycero-3-phosphocholine (DDPC), dihydrocholesterol (DChol), and 27-hydroxycholesterol (27OH) were purchased from Avanti Polar Lipids (Alabaster, AL) and used as received. Texas Red DHPE was purchased from Life Technologies (Carlsbad, CA). Phospholipid/sterol ratio mixtures (70/30) were prepared in chloroform from stock solutions with 0.5 mol % Texas Red DHPE to provide contrast between the coexisting phases and those stored at −22 °C. A spreading solution concentration of 0.5 mg/mL was used for all experiments. The 70/30 phospholipid/sterol ratio is approximately the miscibility critical composition.[12] Finally, to minimize any effects on monolayer oxidation, we replaced cholesterol with dihydrocholesterol, and all images and isotherms were taken within 1 h of monolayer deposition to reduce any photo-oxidative effects.[35,36]

Methods. A known volume of spreading solution was deposited dropwise from a Hamilton syringe (Reno, NV) onto the air−water interface of a Nima 612D Langmuir trough (Coventry, England) filled with water purified to a resistivity of 18 MΩ·cm[2,8,35,36] following extensive aspiration of the interface. The monolayer was allowed to rest with the barriers fully expanded for 10 min to allow for solvent evaporation. Following compression to the desired surface pressure, individual domains were imaged using an Olympus BX-FLA fluorescence microscope coupled to a Retiga EXi CCD camera. To reduce monolayer drift and image distortion, the system was placed in a homemade Faraday cage and placed on a vibration isolation table. The trough and subphase were held at 23 ± 1 °C using a VWR temperature control circulating water bath. The relative humidity was not controlled. The videos were separated into still frames, which were processed using NIH ImageJ routines "Subtract Background", "Enhance Contrast", and "Threshold" to convert to binary (black/white) images. Only domains larger than 50 pixels were counted to avoid errors associated with counting noise; this limited us to domains >1.5 μm in radius. The domain circularity ($4\pi A/P^2$, in which A is the domain area and P the domain perimeter) was limited to between 0.8 and 1.0 to ensure that only circular domains were counted. A Matlab script was written to evaluate the domain areas in square pixels, which were then converted to square micrometers. The fraction of domains of a given radius range was determined by dividing by the number of domains counted. The number of histogram bins was set equal to the square root of the number of domains counted.

The effects of the compression rate on the domain morphology were examined using a Kibron Microtrough X while imaging with an Olympus IX-71 fluorescence microscope. Compression rate images were taken using a Hitachi Flash 2.8 CMOS digital camera. An R&K pressure sensor was used to measure surface pressure because of its fast sampling rate. Secondary nucleation events were induced by a rapid decrease in trough area, which was accompanied by a rapid increase in surface pressure. Eight pictures of the monolayer were taken 10−12 s apart. The aperture was closed between photographs to prevent photobleaching of the fluorescent dye. Movies of the monolayer were taken at 20 fps and saved as TIFF files for analysis with Matlab.

RESULTS AND DISCUSSION

Figure 1 illustrates a typical phase-separated monolayer of 70 mol % DMPC/30 mol % DChol as the surface pressure was increased and the monolayer approached the miscibility phase transition. The dark, typically continuous phase is the liquid-ordered (L_o, cholesterol-rich) phase that excludes the Texas Red DHPE lipid dye, and the bright, discontinuous phase is the liquid-disordered (L_d, cholesterol-poor) phase in which the Texas Red DHPE lipid dye is soluble.[2,30] The fractions of each phase are roughly 50:50% at all surface pressures up to the miscibility transition. Consistent with previous literature

DOI: 10.1021/acs.langmuir.9b01696
Langmuir 2019, 35, 16053−16061

reports, we find the pressure at which the L_o and L_d phases mix to form a single phase to be 8.8 mN/m at room temperature.[2,30] Figure 1 shows that the boundary fluctuations increase as the system approaches the miscibility transition pressure; some domains transition from circles to stripes, which is a sign of near criticality.[2,12,37] The binary nature of the images simplifies the image-processing techniques needed to extract the monolayer line tension[8,14,15,30,33,34] or the domain size distributions.[14,15]

Theory: Boundary Fluctuation Analysis. A series of movies of the monolayer at pressures varying from 5.0 to 8.6 mN/m were collected (Figure 1). This allowed for 450−2700 domains to be tracked at each surface pressure and analyzed by fast Fourier transforms to determine the spectrum of boundary fluctuations.[8] Thermally driven fluctuations drive the domain boundary away from the minimum length/area circular shape given by eq 2 for liquid domains in an immiscible liquid continuous phase (Figure 2A,B). The excess energy of these fluctuations can be described in terms of variations in the apparent domain radius, which increases the domain perimeter compared to the minimal energy or unperturbed circular radius. The line energy contribution to the domain energy is the product of λ and the domain boundary contour length, C. The contour length can be expressed in terms of the radius of the domain as

$$C = \int_0^{2\pi} r\, \partial\phi + \frac{1}{2r_o}\int_0^{2\pi}\left(\frac{\partial r}{\partial\phi}\right)^2 \partial\phi \tag{3}$$

in the case of no overhangs, and the radius, r, is a single-valued function of the polar angle, ϕ[8,38,39] (Figure 2b). The domain radius, $r(\phi)$, can be represented as a Fourier series expansion of the fluctuating interface about the minimum-energy radius, r_0:

$$r(\phi) = r_o\left[1 + \sum_{n=1}^{\infty}(a_n \cos(n\phi) + b_n \sin(n\phi))\right] \tag{4}$$

r_0 is defined as the radius of the circle corresponding to the measured domain area, $A = \pi r_0^2$. Taking the domain to be incompressible and of constant area, A, and by combining eqs 3 and 4, the contour length of the fluctuating domain boundary is

$$C = \int \partial C \cong 2\pi r_o + \frac{\pi r_o}{2}\sum_{n=2}^{\infty}(n^2 - 1)(a_n^2 + b_n^2) \tag{5}$$

The excess energy, ΔF, relative to the minimum circular configuration due to the fluctuations is

$$\Delta F = F - 2\pi r_o\lambda = \frac{\pi r_o\lambda}{2}\sum_{n=2}^{\infty}(n^2 - 1)(a_n^2 + b_n^2) \tag{6}$$

The equipartition theorem states that there is k_BT of energy per mode, which gives

$$\langle a_n^2\rangle + \langle b_n^2\rangle = \frac{2k_BT}{\pi r_o\lambda}\left(\frac{1}{(n^2 - 1)}\right) \tag{7}$$

Equation 7 relates the average values of the Fourier coefficients to the line tension and energy stored in a fluctuating mode. Equation 7 can be recast by setting $y = [\langle a_n^2\rangle + \langle b_n^2\rangle]$, $x = \frac{1}{(n^2-1)}$, and $m = \frac{2k_BT}{\pi r_o\lambda}$. All available Fourier coefficients can be related to the line tension through a linear fit (Figure 2D). In practice, analysis is limited to the largest domains in the monolayer; the greater domain area allows for more precision in the calculation of the domain area, $A = \pi r_0^2$, the magnitude of the fluctuations, and the Fourier coefficients. A possible complication of this practical constraint is that domains with $r_0 \geq e^{1/3} r_o$ (eq 2) are unstable to elliptical or higher-order distortions,[12,24] and the minimum-energy domain shape is no longer circular. As a result, it is important to evaluate only domains with $0.8 < 4\pi A/P^2 < 1$, in which A is the domain area and P is the domain perimeter, to ensure only equilibrium domains were counted. However, the boundary fluctuation method we utilize here does not provide estimates of the dipole density difference, μ, so r_o cannot be determined directly from this analysis.

Theory: Domain Size Distribution Analysis (SD). From the same movies, selected frames were analyzed to extract the domain size distribution: 3600−15 000 individual domains were identified from binary images, and the black domain areas were determined using ImageJ or Matlab software routines.

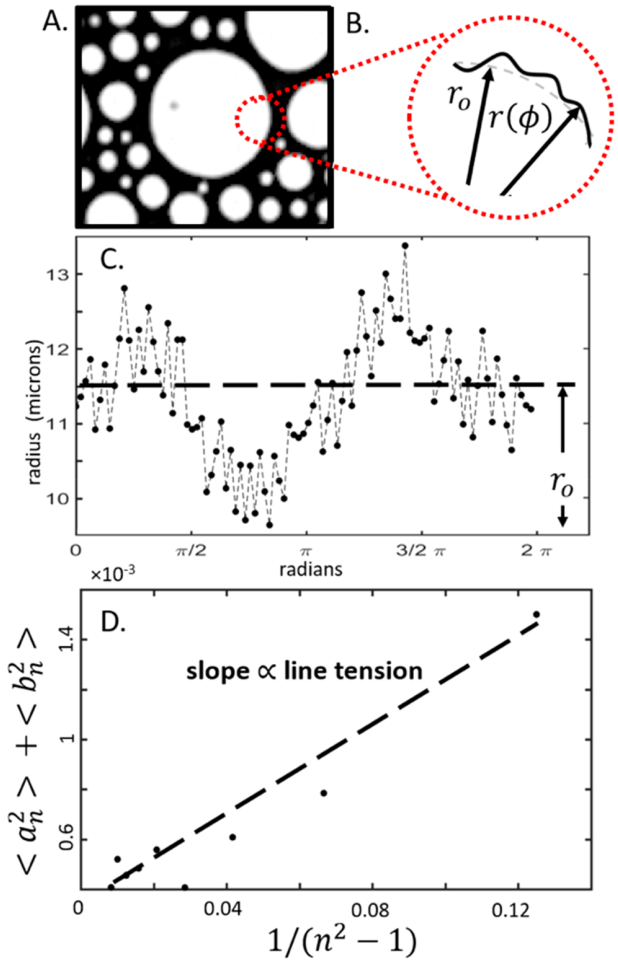

Figure 2. (A) Monolayer image and (B) parametrization of the image to determine the variations in the domain radius, $r(\varphi)$, compared to the mean radius, r_o. (C) Experimental values of $r(\varphi)$. The dotted line is a guide for the eye. The dashed horizontal line represents the average radius, r_o, determined from the domain area, $A = \pi r_o^2$. (D) Fourier coefficients vs mode number plot used to extract the line tension from the slope of the best-fit dashed line via eq 7.

DOI: 10.1021/acs.langmuir.9b01696
Langmuir 2019, 35, 16053−16061

Only domains with areas of 30 pixels or more were counted (radii $\gtrsim$1 μm) to minimize errors associated with counting noise. From the measured domain areas, the domain radius was calculated from $r = (A/\pi)^{1/2}$ and the fraction of domains of a given range of radii (scaled by the total number of domains counted) was binned into histograms. For the initial fit, the number of bins was set equal to the square root of the total number of domains. Representative size distributions are shown in Figure 3.[14,15]

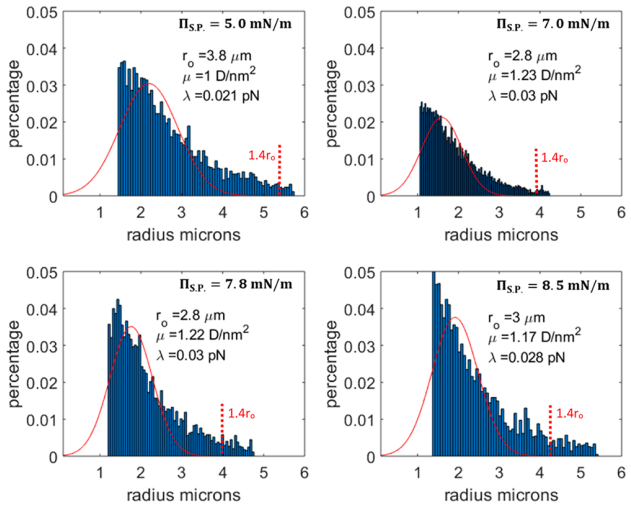

Figure 3. Size distribution histograms and fits for a sample of 70 mol % DMPC/30 mol % DChol are shown at four different surface pressures approaching the transition pressure of 8.8 mN/m. Values of the line tension, λ, the equilibrium radius, r_o, and the dipole density difference, μ, determined from the fit to eq 12 are illustrated. The size distribution does not change significantly with surface pressure, which is reflected in only minor changes in λ, r_o, and μ. Fits and analysis were carried out in Matlab. According to the stability analysis, domains larger than $e^{1/3}r_o \approx 1.4r_o$ should be unstable to elliptical or higher-order distortions. However, the measured size distribution shows a substantial fraction larger than $1.4r_o$ (dotted red lines), suggesting that the size distribution is not at equilibrium.

The domains are polydisperse, and there is no obvious preferred domain radius as suggested by eq 2, which suggests that the entropy of mixing makes a substantial contribution to the equilibrium distribution. To describe an "equilibrium" distribution, we equate the chemical potential of a molecule of area a_0 in a liquid-ordered (L_o) domain of M molecules, corresponding to r_o in eq 2 ($M = \pi r_o^2/a_o$), to that of a molecule in a similar domain of N molecules of radius r ($N = \pi r^2/a_o$)

$$\mu_N^0 + \frac{k_B T}{N}\ln\frac{X_N}{N} = \mu_M^0 + \frac{k_B T}{M}\ln\frac{X_M}{M} \tag{8}$$

in which μ_N^0, X_N and μ_M^0, X_M are the standard-state chemical potentials and mole fractions of molecules in domains of sizes N and M, respectively. This ideal mixing entropy used in eq 8 assumes no interactions between domains. This may be overly simplified because long-range interactions between domains prevent the domains from coalescing, requiring domain size changes to occur by molecular diffusion between domains. Equation 8 can be rearranged to describe the number fraction of domains, $C_N = X_N/N$ and $C_M = X_M/M$, the fractions of domains with N (radius r) or M (radius r_o) molecules, respectively,

$$C_N = \left[C_M \exp\left(\frac{M(\mu_M^0 - \mu_N^0)}{k_B T}\right)\right]^{N/M} = \left[C_M \exp\left(\frac{\pi r_0^2(\mu_M^0 - \mu_N^0)}{a_0 k_B T}\right)\right]^{r^2/r_0^2} \tag{9}$$

For $(\mu_M^0 - \mu_N^0)$ we use a quadratic Taylor series expansion of eq 1 around r_0 to determine the energy difference between domains of N or M molecules:[14]

$$\mu_M^0 - \mu_N^0 = \frac{a_0\mu^2}{r_0}\left(\frac{1}{r} - \frac{1}{r_0}\right)^2 \tag{10}$$

The Taylor series expansion is an excellent approximation to the full energy difference around r_o[14,15] and is needed to prevent an unphysical result as $r \to 0$.

Substituting eq 10 into eq 9 gives

$$C_N = \left[C_M \exp\left(-\frac{\pi\mu^2 r_0\left(\frac{r_0}{r-1}\right)^2}{k_B T}\right)\right]^{r^2/r_0^2} \tag{11}$$

Equation 11 is used to fit the domain size distribution (Figure 3) using C_M, $\beta = \frac{\pi\mu^2 r_0}{k_B T}$, and r_0 as the three fitting parameters:

$$C_N = \left[C_M \exp\left(-\beta\left(\frac{r_0}{r-1}\right)^2\right)\right]^{r^2/r_0^2} \tag{12}$$

C_M is the value of the distribution at r_o; β is related to the width of the distribution, but the three parameters are not independent and are adjusted to best fit the data as well as to approximately normalize the probability distribution. The line tension, λ, and the dipole density difference, μ, are obtained from the fit of the size distributions to eq 12, $\mu^2 = \beta k_B T/\pi r_0$, and from eq 2, $\lambda = \mu^2 \ln(4r_0/e^3\delta)$. Values of the parameters can be checked for internal consistency; for example, C_M is the concentration at $r = r_0$ which gives a check of the values of the fitting parameters. A second check can be obtained by determining the location of the maximum in the distribution:

$$\frac{\partial C_N}{\partial\left(\frac{r}{r_0}\right)} = \frac{\partial}{\partial\left(\frac{r}{r_0}\right)}C_N = \frac{\partial}{\partial\left(\frac{r}{r_0}\right)}\left[C_M \exp\left(-\beta\left(\frac{r_0}{r-1}\right)^2\right)\right]^{r^2/r_0^2} = 0$$

$$\frac{r_{max}}{r_0} = \frac{\beta}{\beta - \ln(C_M)} = \frac{1}{1 - \frac{[k_B T \ln(C_M)]}{(\pi\mu^2 r_0)}} < 1 \tag{13}$$

The entropy of mixing makes the most probable radius $r_{max} < r_o$ for $C_M < 1$. Figure 3 shows that r_{max} for the distributions is between 1 and 2 μm, and r_o is between 2.8 and 3.8 μm.

The experimental domain size distribution does not include data for domains with radii of <1 μm because smaller domains were beyond the resolution of the fluorescence microscope

DOI: 10.1021/acs.langmuir.9b01696
Langmuir 2019, 35, 16053−16061

used. However, stability analysis shows that circular domains with $r \leq r_o/e$ are unstable with respect to coalescence,[40,41] so no equilibrium domains are possible for $r \leq 0.37r_o$. We added equal-width bins with domain fraction equal to zero over the range $0 < r < 0.37r_o$ to the histogram to give a better representation of the actual size distribution and force the fit to zero at $r = 0$. This requires an iterative fit to the histogram to get a preliminary value of r_o, which is then refined in subsequent fits. This theoretically justified fitting constraint was not used in previous work.[14,15] Stability analysis has also shown that for an equilibrium distribution the largest domains in the distribution should be no larger than $e^{1/3}r_o(\approx 1.4r_o)$.[12,24] Such domains should undergo elliptical or higher-order distortions and would not be counted. However, the histograms in Figure 3 show that the fit is not good for domain sizes greater than r_o, and we find a significant fraction of the domains larger than $1.4r_o$ (dotted red lines in Figure 3a–d), which suggests that the size distribution is likely still evolving during the experiment. Larger domain sizes are consistent with a larger value of the line tension from eq 2.

Experimental Results. Figure 4A shows a log–log plot of the measured line tension determined by boundary analysis of domain fluctuations (BA, squares) and domain size distribution analysis (SD, circles) as a function of the reduced pressure, $\pi_R = (\pi_c - \pi)/\pi_c$. (Tabulated values of the line tension and dipole density difference are in the Supporting Information.) π_R is the normalized difference between the critical miscibility pressure, $\pi_c = 8.8$ mN/m, and the measured surface pressure, π, scaled by π_c. The BA data shows a linear decrease in the measured line tension from ~0.4 to ~0.05 pN as the critical miscibility pressure is approached, with a slope of 0.81 ± 0.05, in good agreement with previous measurements of the line tension for DMPC–cholesterol mixtures.[10,11,13,30,42] However, the line tension measured by the SD technique gave an effectively constant and much lower value of ~0.02–0.03 pN for the line tension, which did not depend on the reduced surface pressure. The dipole density difference also varied little with surface pressure and ranged from 1.0 to 1.2 D/nm^2. This is consistent with the lack of change in the most probable domain radius, which varied from 2.8 to 3.8 μm, and the overall size distribution of the domains shown in Figure 3. Previous results of Israelachvili and co-workers[14,15] also showed a minimal dependence of λ and μ on surface pressure. However, our measurements of λ are an order of magnitude larger than previous results from size distribution measurements,[14,15] which we attribute to constraining the fit to zero for domains of $r < 0.37r_o$. However, we expected the domain size distribution to change as the critical miscibility pressure was approached because the line tension and dipole density difference have different scaling properties near the critical point as evidenced by the well-known circle to stripe domain shape transition.[2,10,11,23,29,30]

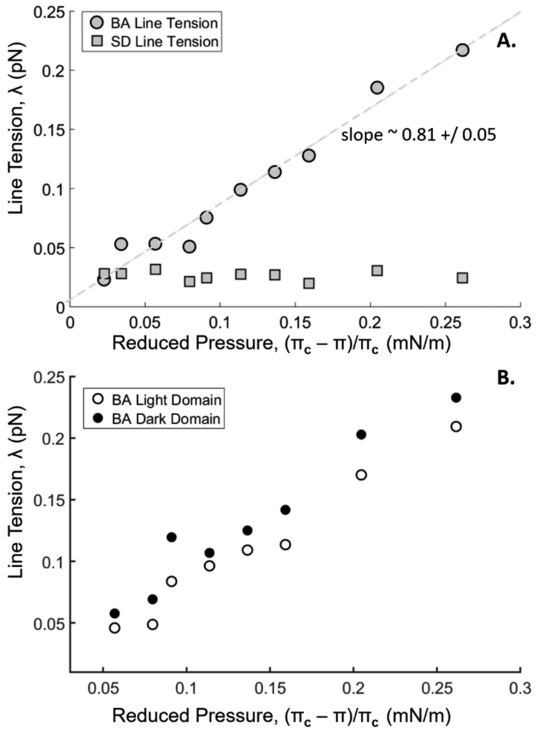

Figure 4. (A) Line tensions measured by BA (squares) and SD (circles) as a function of the reduced surface pressure. The BA data shows a linear increase with reduced surface pressure consistent with the theoretical critical exponent, $\varphi \approx 1$. (See Figure 5.) The SD data is independent of surface pressure and is significantly lower. (B) Experimental values of line tension as a function of reduced surface pressure ($\pi_c = 8.8$ mN/m) by the BA method for 70:30 mol %/mol% DMPC/dihydrocholesterol. Solid circles are for L_d domains in an L_o matrix, and open circles are for L_o domains in an L_d matrix. The line tensions for both sets of domains are equal within experimental error. Both sets of data are linear in reduced surface pressure, consistent with critical scaling with a critical exponent of $\varphi \approx 1$.

Theory suggests that when approaching the critical miscibility surface pressure from below, the line tension can be expressed as a power law function of the reduced surface pressure $\lambda = a\pi_R^{\phi}$.[10,11,13,30,42] Here, $\phi = (d-1)\nu$, in which $\nu = 1$ is the critical exponent for the correlation length of the 2-D Ising universality class, d is the number of dimensions in the system, and a is a constant that depends on the system.[10,11,13,30,42] For monolayers, $d = 2$, which gives the prediction that $\phi = 1$, which is consistent with the results for the BA method in Figure 4A of $\phi = 0.84 \pm 0.05$. Previous measurements of ϕ are also ~1 for both monolayer and bilayer systems of similar lipids.[10,11,13,30,42] For the SD method, the data show an invariance with reduced surface pressure, which implies a critical exponent, $\phi \approx 0$, inconsistent with previous work and theoretical predictions for the critical immiscibility transition.

Figure 4B shows that the line tension was the same within experimental error when evaluated by the BA method using the fluctuations of liquid-ordered domains (dark domains in Figure 1) in a liquid-disordered matrix or the fluctuations of the liquid-disordered domains (light domains in Figure 1) in a liquid-ordered matrix. The good agreement between these "light" and "dark" results is consistent with theory, and the difference in interfacial tension between the light and dark phases provides an experimental check on the image-processing routines.

The constant line tension measured by the SD technique is consistent with the lack of change in the domain size distribution in Figure 3. For this near-critical system in which the fraction of light and dark domains remains about 50:50, the domain size distribution seems to be set by the initial nucleation and growth kinetics of the separate phases rather than equilibrium. Surprisingly, the low and invariant range of line tensions suggested by the SD method for this

DOI: 10.1021/acs.langmuir.9b01696
Langmuir 2019, 35, 16053–16061

critical mixture of DMPC and dihydrocholesterol was similar to those measured for model myelin lipids (L_o–L_d liquid phases, as is the case here)[14] and model lung surfactant lipids with and without the lung surfactant specific protein SP-B (liquid condensed–liquid expanded phase coexistence)[15] measured by the SD technique. The previous results for the line tension measured by the SD technique also showed a minimal dependence on surface pressure[14,15] and did not show the expected critical scaling behavior for the myelin lipid system.[14]

Figure 5 shows the experimental line tensions (measured using the BA method) of three phosphatidylcholines of

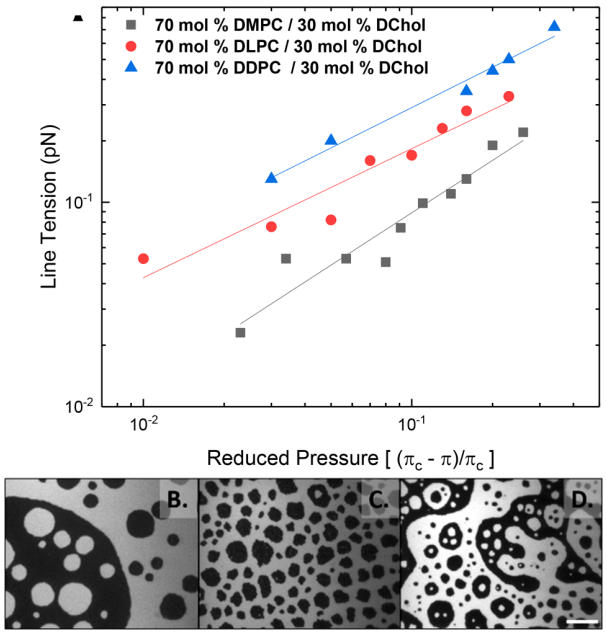

Figure 5. (A) Line tension measured for a series of phosphatidylcholine (PC)/dihydrocholesterol mixtures of varying PC chain length: DDPC (10 carbons), DLPC (12 carbons), and DMPC (14 carbons). Line tensions are plotted against the reduced pressure of each lipid mixture. Transition pressures for DDPC, DLPC, and DMPC are 22.6, 15.5, and 8.8 mN/m. Representative panels illustrate monolayers of 70 mol %. All three mixtures are consistent with the critical scaling relationship, $\lambda = a\pi_R^{\phi}$, with $\varphi = 0.69 \pm 0.07$ for DDPC and DLPC and $\varphi = 0.84 \pm 0.09$ for DMPC. The prefactor, a, increases with decreasing chain length; for DDPC, $a = 1.4$; for DLPC, $a = 0.89$; and for DMPC, $a = 0.61$. (B) DDPC/DChol 70:30 monolayer at 22.1 mN/m. (C) DLPC/D Chol 70:30 monolayer at 15.0 mN/m and (D) DMPC/DChol 70:30 monolayer at 8.1 mN/m and $\varphi = 0.69 \pm 0.07$ for DDPC and DLPC and $\varphi = 0.84 \pm 0.09$ for DMPC within the experimental error. The prefactor, a, increases with decreasing chain length; for DDPC, $a = 1.4$, and for DLPC, a shows similar monolayer phase separation and fluctuating domain shapes in these three mixtures. The scale bar is 25 μm.

different chain lengths (DDPC, 10 carbon chains; DLPC, 12 carbon chains; and DMPC, 14 carbon chains) in 70:30 mol/mol mixtures with dihydrocholesterol as a function of the reduced surface pressure, π_R. The critical miscibility transition pressures for DDPC, DLPC, and DMPC are 22.6, 15.5, 8.8 mN/m, respectively. Figure 5 shows that all three mixtures are consistent with the critical scaling relationship, $\lambda = a\pi_R^{\phi}$, with = 0.89, and for DMPC, $a = 0.61$, likely reflecting the increasing critical miscibility surface pressures with decreasing chain length.

METASTABLE VS EQUILIBRIUM DOMAIN SIZE DISTRIBUTIONS

The histogram of domain size distributions in Figure 3 showed little variation with surface pressure or reduced surface pressure, which would suggest that the domains are kinetically trapped in a metastable state due to the monolayer history. Figure 6A shows the effect of compression speed on the size

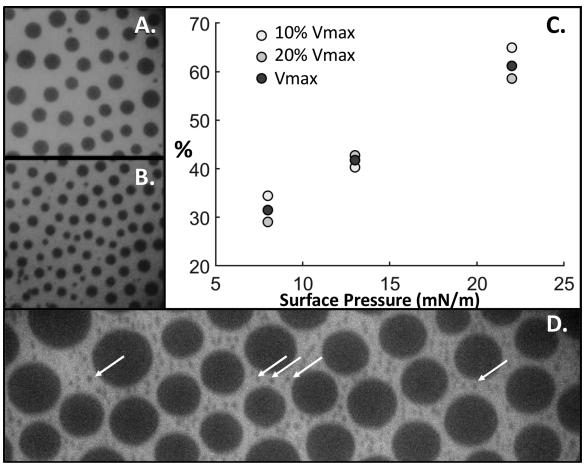

Figure 6. Results of compression rates for monolayers of 27OH/DMPC monolayers (30:70). Monolayer compressed at (A) $0.2V_{max}$ and (B) V_{max} (140 mm/min). Domains were roughly a factor of 2 larger at the slower compression rate. (C) The net percentage (%) of dark domains was effectively constant and independent of the compression rate, suggesting that the composition of the domains reaches equilibrium much faster than the size distribution. (D) Fluorescent images of a dual population of 27OH domains formed in two nucleation events due to an increase in the compression rate. The larger domains were formed by compressing the monolayer at a speed of 14 mm/min, and the smaller domains (arrows) were formed when the compression speed was increased to 140 mm/min. The small L_o domains persisted for 30 min before dissolving into the L_d phase.

distribution of mixtures of DMPC with 27-hydroxycholesterol. 27-Hydroxycholesterol–DMPC mixtures were used as the domain sizes were more monodisperse than for dihydrocholesterol–DMPC mixtures, which helps highlight the changes in the size distribution. Changing the compression rate from the maximum compression speed for our trough, V_{max}(140 mm/min), to 20% of the maximum speed, $0.2V_{max}$ (28 mm/min), increased the average domain size by a factor of 2. However, Figure 6B shows that there is little change in the dark domain area fraction depending on compression rates, suggesting that the composition of the domains has likely reached equilibrium following the initial nucleation event. The initial nucleation of phase-separated domains is rapid, but the domain size distribution is likely kinetically trapped as a result of the slow diffusional equilibration time and the strong electrostatic repulsion between domains that prevents domain coalescence.[32] (The coalescence of domains in bilayers is much more facile because the dipole repulsion between domains in each monolayer leaflet is canceled by the other leaflet, which has the opposite orientation of the dipoles.) Figure 6C shows that while large domains were grown by compression at 14 mm/min, briefly increasing the compression rate to 140 mm/min nucleated a new set of domains; the freshly nucleated domains persisted for 30 min. Previous work by Israelachvili and coworkers has shown that the domain size distribution in similar

DOI: 10.1021/acs.langmuir.9b01696
Langmuir 2019, 35, 16053–16061

DMPC−DChol mixtures continues to evolve for 60 h or more, with the domains slowly growing larger and the size distribution narrowing with time.[43] Larger and more monodisperse domains would cause the SD method to predict an increase in the line tension toward the values measured by the BA method. The effect of monolayer history on the domain size distribution will be examined in future work.

CONCLUSIONS

The composition and surface pressure dependences of the magnitudes of the line tension, λ (the two-dimensional analog of the surface tension[12,18]), and the dipole density difference, μ, are essential to understanding the evolution of the morphology of phase-separated phospholipid−cholesterol monolayers and bilayers.[2,5−7,9,12,13,16,23,27,30,34,42,44,45] The magnitudes of λ and μ are also essential to the stability of membrane rafts that provide sites for specific protein localization.[1,3,16] An analysis of domain boundary fluctuations (BA) in three phospholipid−dihydrocholesterol mixtures shows that the magnitude of λ increases from 0.05 to 0.4 pN for 70 mol % PC−30 mol % dihydrocholesterol monolayers as the reduced pressure, π_R, is increased. The line tension scales for three different saturated phosphatidylcholine−dihydrocholesterol mixtures are predicted for a two-dimensional Ising model with $\lambda = a\pi_R^{\phi}$, with $\phi \approx 1$ consistent with previous investigations.[13,30]

The BA method does not provide a direct estimate of the dipole density difference. However, while the size distributions in Figure 3 are likely metastable, they are sharply peaked at a radius of ∼2.5 μm for all surface pressures examined. If we set this most probable radius equal to r_0 in eq 2, then we can estimate the dipole density difference to be $\mu = 0.3$ D/nm^2 for $\lambda = 0.05$ pN near the critical miscibility surface pressure and $\mu = 0.6$ D/nm^2 for $\lambda = 0.22$ pN far from the critical miscibility surface pressure.[11,14,30] These values are consistent with previous literature estimates of μ of ∼1 D per molecule in which the area/molecule in these monolayers is ∼0.5 nm^2.[11,30] This is about half the value of μ determined from the SD method.

The line tensions determined by domain size distribution analysis (SD)[14,15] for the same 70 mol % DMPC−30 mol % dihydrocholesterol mixture were effectively constant as a function of surface pressure, as were the domain size distributions themselves. The magnitude of λ determined by the SD method was significantly smaller than that determined by the BA method and ranged from 0.02 to 0.03 pN. This is likely because the size distribution of monolayer domains is metastable and is initially determined by the kinetics of domain nucleation and subsequent monolayer history. Equilibration of the domain sizes by the coalescence of smaller domains is strongly inhibited by dipole−dipole repulsion. This requires equilibration by Ostwald ripening or the "evaporation" of molecules from high-energy domains followed by condensation onto lower-energy domains,[34] which is a lengthy process and likely does not occur over experimentally accessible time scales,[32] especially when the difference in energy between molecules in different domains is small compared to k_BT.[43] In addition to the work of Hu et al.[43] that showed that the domain size distribution of DMPC−cholesterol mixtures evolved over 60 h, McConlogue and Vanderlick demonstrated that the compression hysteresis and nucleation time modulate the shape of DPPC domains.[46,47] Seul et al.[32] showed that the domain size distribution in off-critical mixtures of DMPC and dihydrocholesterol evolved for up to 90 h. Similar to Figure 6, Nag et al. have shown that the DPPC domain size distribution is strongly dependent on compression rates.[48] However, as the line tension measured by the BA method is consistent between a number of experimental methods and laboratories (Table 1), it appears that the composition of the domains likely reaches equilibrium much faster than the size distribution. The BA method succeeds because of the rapid establishment of local equilibrium between the L_o and L_d domains; the time scale for diffusive processes should scale as R^2/D, in which R is the domain radius and D is the lipid diffusivity. For the typical domains in this work, $R \approx 2$ μm in diameter, $D = 4 \times 10^{-8}$ cm^2/s, and this diffusive time scale is ∼1 s, and we expect compositional variations to equilibrate within minutes. However, the SD method requires global equilibrium to be established over the domain size distribution, with the variations in energy per molecule being small between domains of different sizes. This greatly decreases the driving force for diffusive equilibrium, requiring hours to days.[43] Hence, the size distributions evolve too slowly for the SD method to be a reliable method of predicting line tension.

ASSOCIATED CONTENT

Supporting Information

The Supporting Information is available free of charge on the ACS Publications website at DOI: 10.1021/acs.langmuir.9b01696.

Line tensions of 70 mol % DMPC/30 mol % DChol, 70 mol % DLPC/30 mol % DChol, and 70 mol % DDPC/30 mol % DChol (PDF)

AUTHOR INFORMATION

Corresponding Author

*E-mail: stottrup@augsburg.edu.

ORCID

Benjamin L. Stottrup: 0000-0001-8274-7324

Joseph A. Zasadzinski: 0000-0001-5663-6989

Notes

The authors declare no competing financial interest.

ACKNOWLEDGMENTS

We thank Ravi Tavakley and members of Augsburg Biophysics. We thank Emil Eldo and Promise Okeke for preliminary experiments performed in support of this project. Research in Augsburg's biophysics laboratory is supported by the National Science Foundation: DMR 1207544 and MRI 1040126. We thank Dixie Shafer, Kirsten O'Brien, and Augsburg University's Office of Undergraduate Research and Graduate Opportunities. Undergraduate researchers acknowledge the support of summer research stipends from Dean and Amy Sundquist. J.A.Z. and B.L.S. were partially supported by National Institutes of Health grants HL 51177 and HL 135065 and NSF grant CBET 1706378.

REFERENCES

(1) Simons, K.; Ikonen, E. Functional rafts in cell membranes. *Nature* **1997**, *387*, 569−572.

(2) Keller, S. L.; McConnell, H. M. Stripe phases in lipid monolayers near a miscibility critical point. *Phys. Rev. Lett.* **1999**, *82*, 1602−1605.

(3) Lingwood, D.; Simons, K. Lipid rafts as a membrane-organizing principle. *Science* **2010**, *327*, 46−50.

DOI: 10.1021/acs.langmuir.9b01696
Langmuir 2019, 35, 16053−16061

(4) Veatch, S. L. From small fluctuations to large-scale phase separation: lateral organization in model membranes containing cholesterol. *Semin. Cell Dev. Biol.* **2007**, *18*, 573−582.
(5) Veatch, S. L.; Keller, S. L. Organization in lipid membranes containing cholesterol. *Phys. Rev. Lett.* **2002**, *89*, 268101.
(6) Veatch, S. L.; Keller, S. L. Separation of liquid phases in giant vesicles of ternary mixtures of phospholipids and cholesterol. *Biophys. J.* **2003**, *85*, 3074−3083.
(7) Veatch, S. L.; Keller, S. L. Seeing spots: complex phase behavior in simple membranes. *Biochim. Biophys. Acta, Mol. Cell Res.* **2005**, *1746*, 172−185.
(8) Stottrup, B. L.; Heussler, A. M.; Bibelnieks, T. A. Determination of line tension in lipid monolayers by Fourier analysis of capillary waves. *J. Phys. Chem. B* **2007**, *111*, 11091−11094.
(9) Baumgart, T.; Hess, S. T.; Webb, W. W. Imaging coexisting fluid domains in biomembrane models coupling curvature and line tension. *Nature* **2003**, *425*, 821−824.
(10) Benvegnu, D. J.; McConnell, H. M. Line tension between liquid domains in lipid monolayers. *J. Phys. Chem.* **1992**, *96*, 6820−6824.
(11) Benvegnu, D. J.; McConnell, H. M. Surface dipole densities in lipid monolayers. *J. Phys. Chem.* **1993**, *97*, 6686−6691.
(12) McConnell, H. M. Structures and Transitions in Lipid Monolayers at the Air-Water-Interface. *Annu. Rev. Phys. Chem.* **1991**, *42*, 171−195.
(13) Honerkamp-Smith, A. R.; Cicuta, P.; Collins, M. D.; Veatch, S. L.; den Nijs, M.; Schick, M.; Keller, S. L. Line tensions, correlation lengths, and critical exponents in lipid membranes near critical points. *Biophys. J.* **2008**, *95*, 236−246.
(14) Lee, D. W.; Min, Y.; Dhar, P.; Ramachandaran, A.; Israelachvili, J. N.; Zasadzinski, J. A. Relating Domain Size Distribution to Line Tension and Molecualr Dipole Density in Model Cytoplasmic Lipid Monolayers. *Proc. Natl. Acad. Sci. U. S. A.* **2011**, *108*, 9425−9430.
(15) Dhar, P.; Eck, E.; Israelachvili, J. N.; Lee, D. W.; Min, Y.; Ramachandaran, A.; Waring, A. J.; Zasadzinski, J. A. Lipid-protein interactions alter line tensions and domain size distributions in lung surfactant monolayers. *Biophys. J.* **2012**, *102*, 56−65.
(16) Rayermann, S. P.; Rayermann, G. E.; Cornell, C. E.; Merz, A. J.; Keller, S. L. Hallmarks of Reversible Separation of Living, Unperturbed Cell Membranes into Two Liquid Phases. *Biophys. J.* **2017**, *113*, 2425−2432.
(17) Trabelsi, S.; Zhang, S.; Lee, T. R.; Schwartz, D. K. Linactants: Surfactant analogues in two dimensions. *Phys. Rev. Lett.* **2008**, *100*, 037802.
(18) Sriram, I.; Schwartz, D. K. Line tension between coexisting phases in monolayers and bilayers of amphiphilic molecules. *Surf. Sci. Rep.* **2012**, *67*, 143−159.
(19) Mann, E. K.; Henon, S.; Langevin, D.; Meunier, J.; Leger, L. Hydrodynamics of domain relaxation in a polymer monolayer. *Phys. Rev. E: Stat. Phys., Plasmas, Fluids, Relat. Interdiscip. Top.* **1995**, *51*, 5708−5720.
(20) Stone, H. A.; McConnell, H. M. Hydrodynamics of quantied shape transitions of lipid domains. *Proc. R. Soc. London, Ser. A* **1995**, *448*, 97−111.
(21) Weis, R. M.; McConnell, H. M. Two-dimensional chiral crystals of phospholipid. *Nature* **1984**, *310*, 47−49.
(22) Keller, D. J.; McConnell, H. M.; Moy, V. T. Theory of superstructures in lipid monolayer phase transitions. *J. Phys. Chem.* **1986**, *90*, 2311−2315.
(23) Keller, S. L.; Pitcher, W. H. I.; Huestis, W. H.; McConnell, H. M. Red Blood Cell Lipids form Immisible Liquids. *Phys. Rev. Lett.* **1998**, *81*, 5019−5022.
(24) Lee, K. Y. C.; McConnell, H. M. Quantized symmetry of liquid monolayer domains. *J. Phys. Chem.* **1993**, *97*, 9532−9539.
(25) Stone, H. A.; McConnell, H. M. Lipid domain instabilities in monolayers overlying sublayers of finite depth. *J. Phys. Chem.* **1995**, *99*, 13505−13508.
(26) Lauger, J.; Robertson, C. R.; Frank, C. W.; Fuller, G. G. Deformation and relaxation processes of mono- and bilayer domains of liquid crystalline Langmuir films on water. *Langmuir* **1996**, *12*, 5630−5635.
(27) Tian, A. W.; Johnson, C.; Wang, W.; Baumgart, T. Line tension at fluid membrane domain boundaries measured by micropipette aspiration. *Phys. Rev. Lett.* **2007**, *98*, 208102.
(28) Lee, K. Y. C.; Klingler, J. F.; McConnell, H. M. Electric-field-induced concentration gradients in lipid monolayers. *Science* **1994**, *263*, 655−658.
(29) Esposito, C.; Tian, A.; Melamed, S.; Johnson, C.; Tee, S. Y.; Baumgart, T. Flicker spectroscopy of thermal lipid bilayer domain boundary fluctuations. *Biophys. J.* **2007**, *93*, 3169−3181.
(30) Heinrich, M. C.; Levental, I.; Gelman, H.; Janmey, P. A.; Baumgart, T. Critical exponents for line tension and dipole density difference from lipid monolayer blundary fluctuations. *J. Phys. Chem. B* **2008**, *112*, 8063−8068.
(31) Israelachvili, J. N. *Intermolecular and Surface Forces*, 2nd ed.; Academic Press: London, 1992.
(32) Seul, M.; Morgan, N. Y.; Sire, C. Domain coarsening in a 2-D binary mixture - growth dynamics and spatial correlations. *Phys. Rev. Lett.* **1994**, *73*, 2284−2287.
(33) Seul, M. Dynamics of domain shape relaxationb in Langmuir films. *J. Phys. Chem.* **1993**, *97*, 2941−2945.
(34) Stanich, C. A.; Honerkamp-Smith, A. R.; Putzel, G. G.; Warth, C. S.; Lamprecht, A. K.; Mandal, P.; Mann, E.; Hua, T. A. D.; Keller, S. L. Coarsening Dynamics of Domains in Lipid Membranes. *Biophys. J.* **2013**, *105*, 444−454.
(35) Stottrup, B. L.; Hernandez-Balderrama, L. H.; Kunz, J. C.; Nguyen, A. H.; Sonquist, B. J. Comparison of Cholesterol and 25-Hydroxycholesterol in Phase-Separated Langmuir Monolayers at the Air-Water Interface. *J. Phys. Chem. B* **2014**, *118*, 11231−11237.
(36) Stottrup, B. L.; Nguyen, A. H.; Tuzel, E. Taking another look with fluorescence microscopy: Image processing techniques in Langmuir monolayers for the twenty-first century. *Biochim. Biophys. Acta, Biomembr.* **2010**, *1798*, 1289−1300.
(37) Min, Y.; Alig, T. F.; Lee, D. W.; Boggs, J. M.; Israelachvili, J. N.; Zasadzinski, J. A. Critical and off-critical miscibility transitions in model extracellular and cytoplasmic myelin lipid monolayers. *Biophys. J.* **2011**, *100*, 1490−1498.
(38) Tuzel, E.; Pan, G.; Ihle, T.; Kroll, D. M. Mesoscopic model for the fluctuating hydrodynamics of binary and ternary mixtures. *EPL* **2007**, *80*, 40010.
(39) Tuzel, E.; Pan, G. A.; Kroll, D. M. Dynamics of thermally driven capillary waves for two-dimensional droplets. *J. Chem. Phys.* **2010**, *132*, 174701.
(40) McConnell, H. M.; Moy, V. T. Shapes of finite two-dimensional lipid domains. *J. Phys. Chem.* **1988**, *92*, 4520−4525.
(41) Lee, K. Y. C.; Klingler, J. F.; McConnell, H. M. Electric-field induced concentration gradients in lipid monolayers. *Science* **1994**, *263*, 655−658.
(42) Honerkamp-Smith, A. R.; Veatch, S. L.; Keller, S. L. An introduction to critical points for biophysicists; observation of compositional heterogeneity in lipid membranes. *Biochim. Biophys. Acta, Biomembr.* **2009**, *1788*, 53−63.
(43) Hu, Y. F.; Meleson, K.; Israelachvili, J. Thermodynamic equilibrium of domains in a two-component Langmuir monolayer. *Biophys. J.* **2006**, *91*, 444−453.
(44) McConnell, H. M.; Tamm, L. K.; Weis, R. M. Periodic structures in lipid monolayer phase transitions. *Proc. Natl. Acad. Sci. U. S. A.* **1984**, *81*, 3249−3253.
(45) McConnell, H. M.; Vrljic, M. Liquid-liquid immiscibility in membranes. *Annu. Rev. Biophys. Biomol. Struct.* **2003**, *32*, 469−492.
(46) McConlogue, C. W.; Vanderlick, T. K. A close look at domain formation in DPPC monolayers. *Langmuir* **1997**, *13*, 7158−7164.
(47) McConlogue, C. W.; Vanderlick, T. K. Molecular determinants of lipid domain shape. *Langmuir* **1999**, *15*, 234−237.
(48) Nag, K.; Boland, C.; Rich, N.; Keough, K. M. W. Epifluorescence microscopic observation of monolayers of DPPC - dependence of domain size on compression rates. *Biochim. Biophys. Acta, Biomembr.* **1991**, *1068*, 157−160.

DOI: 10.1021/acs.langmuir.9b01696
Langmuir 2019, 35, 16053−16061